

An improved spatial-dependent model of neutron multiplicity counting for large-volume plutonium solution

Jia-Cheng Wang,^{1,2} Xiao-Dong Huo,² Hai-Feng Yang,^{2,*} Zeng Shao,² and Kan Wang¹

¹Department of Engineering Physics, Tsinghua University, Beijing 100084, China

²China Nuclear Power Engineering Co., Ltd., Beijing 100084, China

Neutron multiplicity counting is a non-destructive, passive technique for monitoring plutonium inventory. However, when extending the application from plutonium metal/plutonium oxides to large-volume plutonium solution systems, the original “point model” reveals significant shortcomings. Currently, while two types of improvements for original “point model” has been proposed: (a) improved “point model” suitable for small-volume solution systems and (b) volume-weighted “point model” correcting for spatial dependence of solid systems, neither is suitable for large-volume solution systems. Based on the improved “point model”, we firstly employ the volume-weighted approach to derive a volume-weighted model suitable for solution systems, which however neglects the disparity between the induced fission source distribution and the initial source distribution in our opinion. Furthermore, by additionally incorporating the distribution of induced fission reactions as a weighting coefficient for the spatial dependence correction factor, we propose the composite-weighted model. Comparative analysis of simulation results from the improved “point model”, volume-weighted model, and composite-weighted model demonstrates that the composite-weighted model has the best performance, offering superior universality and accuracy, thereby confirming the necessity and validity of the improvements. Theoretically, the methodology for addressing spatial dependence in large-volume solution systems introduced in this study can also be extended to other large-volume plutonium-containing material systems.

Keywords: neutron multiplicity counting, large-volume solution system, spatial dependence correction, composite-weighted model

I. INTRODUCTION

Driven by the needs of nuclear safeguards and arms verification, neutron multiplicity analysis technology has been a major research focus in recent decades. Originally developed for analyzing plutonium in metallic, oxide, debris, and waste forms, this technology is now being extended to other plutonium-based systems, such as plutonium solutions. K. Boehnel’s “point model” provides the foundational principles for neutron multiplicity counting [1]. By solving the equation system of S , D , and T (singles, doubles, and triples rates), one can determine the effective mass of ^{240}Pu , the ratio of (α, n) source neutrons to spontaneous fission neutrons, and the leakage multiplication factor. Detailed descriptions of neutron multiplicity counting methods can be found in references [2–4]. The “point model” is characterized by its use of lumped parameters, treating the entire multiplication system as a single point, thereby neglecting neutron transport within the system and considering only a single energy group. This approach simplifies the equations and makes them easier to compute, but it also has limitations for applications. The establishment of the “point model” relies on certain assumptions that are only well met by small-volume plutonium metal or plutonium oxide samples [5], especially meeting the scenario of nuclear safeguards and arms verification.

For plutonium solution systems, neutron multiplicity counting can also be used to detect the plutonium inventory. However, the fission multiplication process in solution systems differs significantly from that in plutonium metal systems, necessitating corrections to the original “point model”

equations. There are three main differences:

1. In addition to spontaneous fission sources, the solution also contains non-negligible (α, n) neutron sources. This is because after α decay of plutonium, α particles react with oxygen and nitrogen in the solution, resulting in (α, n) neutrons.
2. The strong neutron moderation effect of water significantly reduces the neutron mean free path in the solution. This results in pronounced spatial dependence, causing substantial variations in neutron multiplication factors and detection efficiencies across different positions in the solution.
3. The neutron capture non-fission probability of water cannot be ignored. Therefore, it is necessary to distinguish between the net multiplication factor and the leakage multiplication factor in multiplicity calculations. In plutonium metal, however, the difference between these two factors is small, so there is no need to distinguish between them.

Ref. [5] has already made corrections to “point model” for the first and third differences above, achieving good calculation accuracy in small-volume solution systems.

In research on measuring solid materials, it has been observed that the original “point model” exhibits significant inaccuracies when calculating large-mass and high-multiplication samples. Previous studies [6–10] have identified that the deviation mainly stems from the spatial dependence of multiplication, meaning that neutrons at different positions within the system have different multiplication factors, which is not taken into account in the original “point model”.

* Corresponding author, yanghf@cnpe.cc

An enhanced approach involves incorporating a spatial correction factor based on volume weighting for the multiplication factor, which has yielded promising results in computations for larger-volume plutonium metal samples. This refinement is straightforward and intuitive, although the determination of the spatial correction factor may depend on empirical expression of multiplication factor's distribution [6].

Another model that addresses spatial dependence, akin to the derivation of the "point model", incorporates scattering reactions. It treats scattering as a fission-like event generating a single neutron, while also considering neutron spatial transport and geometric boundaries in Refs. [11–13]. This model offers greater realism and precision than the "point model". However, its complexity increases significantly as the corresponding equations transform from simple algebraic expressions of lumped parameters, to intricate integral equations of microscopic parameters on phase space. Consequently, while it can perform forward calculations (deriving S , D , T from item characteristics), it cannot execute backward solutions (inferring item characteristics from S , D , T). To overcome this limitation, Ref. [14] proposes a neural network-based approach for backward calculations.

Therefore, inspired from the actual physical process, this paper proposes an improved spatial dependence correction method for "point model", forming a more universally applicable spatial-dependent model of neutron multiplicity. To verify the improvement of this model, we set spherical uranium-plutonium solution samples of different radii and a detection device. A three-dimensional Monte Carlo code is used to simulate the corresponding neutron multiplicity counting. By comparative experiments with other improved neutron multiplicity models, we prove that the proposed model can significantly reduce the measurement deviation of plutonium inventory in large-volume solution.

II. POINT MODEL CORRECTION

The original "point model" equations, developed by K. Boehnel, are based on the superfission hypothesis. This model significantly simplifies the complex physical processes by neglecting spatial distributions of system parameters, variations in neutron energy spectra, and neutron capture without fission by the medium. Through these simplifications, it establishes the relationship between neutron multiplicity counting and the factorial moments of the fission neutron multiplicity distribution, represented by equation system of S , D , and T . In this study, we focus exclusively on the first two of these equations for simplicity:

$$S = \varepsilon \nu_{s1} g_{sf}^{240} m_{240}^{eff} M_L (1 + \alpha) \quad (1)$$

$$D = \frac{\varepsilon^2 g_{sf}^{240} m_{240}^{eff} f_D M_L^2}{2} \left[\nu_{s2} + \frac{(M_L - 1)}{\nu_{i1} - 1} \nu_{s1} (1 + \alpha) \nu_{i2} \right] \quad (2)$$

Here, ε signifies the leakage neutron detection efficiency (hereafter referred to as detection efficiency), while g_{sf}^{240}

refers to the spontaneous fission rate of ^{240}Pu , commonly set at 475.276 fission/(g.s). The term m_{240}^{eff} indicates the effective mass of ^{240}Pu , and f_D represents the doubles gate fraction. The parameters ν_{s1} , ν_{s2} , ν_{i1} , and ν_{i2} correspond to the first and second factorial moments of the spontaneous and induced fission neutron multiplicity distributions, respectively. Additionally, α denotes the ratio of (α, n) source neutrons to spontaneous fission source neutrons, and M_L stands for the leakage multiplication factor.

The original "point model" equation system is applicable to measurements involving plutonium metal or plutonium oxides but becomes unsuitable for solution systems containing plutonium. To address this limitation, the original "point model" has been refined in Ref. [5]. Firstly, acknowledging the non-ignorable probability of neutron capture without fission by water, the distinction is introduced between the net multiplication factor M and the leakage multiplication factor M_L . Secondly, as the neutron energy spectrum affects multiplication and detection [15], the multiplication factor and detection efficiency are further subdivided by spectrum. Building on the approach in Ref. [5], the model is further simplified by considering ν_{i1} and ν_{i2} identical across two source terms, which leads to an improved "point model" equation system:

$$S = \nu_{s1} g_{sf}^{240} m_{240}^{eff} (\varepsilon_1 M_{L1} + \alpha \varepsilon_2 M_{L2}) \quad (3)$$

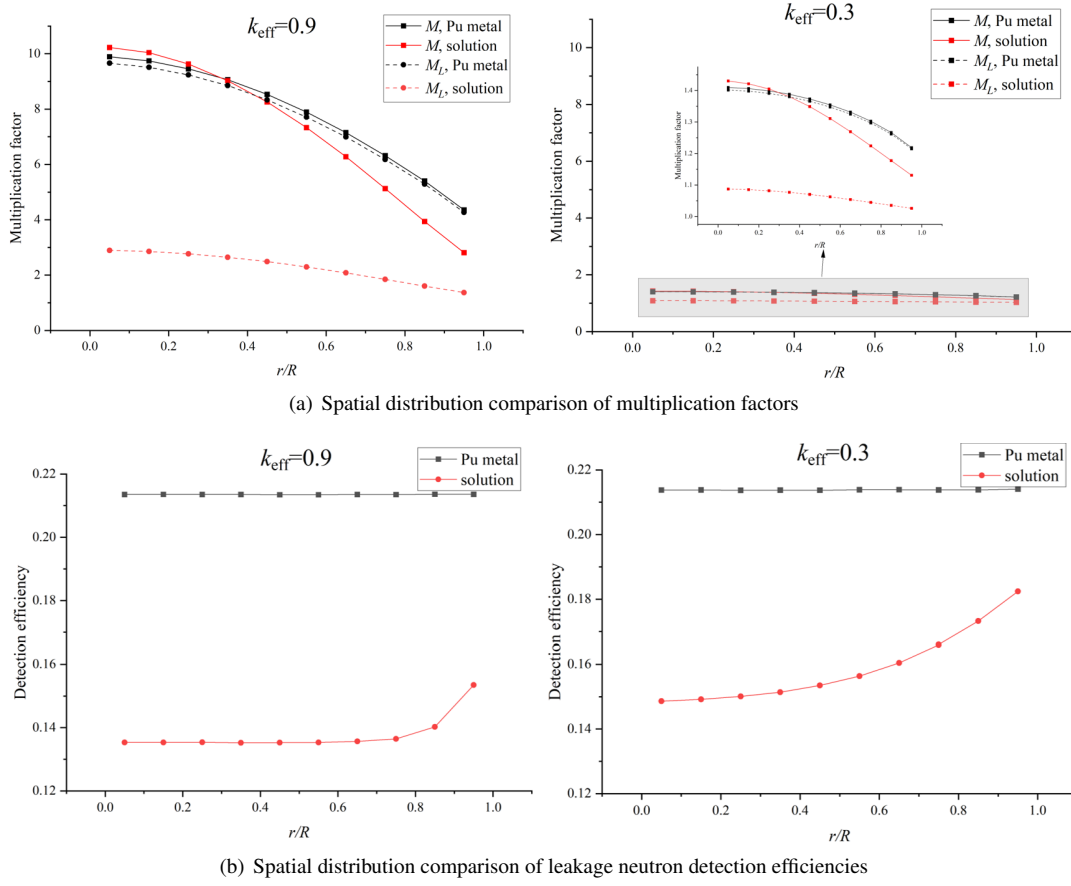
$$D = \frac{g_{sf}^{240} m_{240}^{eff} f_D M_{L1}^2}{2} \left[\varepsilon_1^2 \nu_{s2} + \varepsilon_{id}^2 \frac{(M_1 - 1)}{\nu_{i1} - 1} \nu_{s1} \nu_{i2} + \alpha \varepsilon_{id}^2 \frac{(M_2 - 1)}{\nu_{i1} - 1} \nu_{s1} \nu_{i2} \right] \quad (4)$$

Here, the subscripts 1 and 2 are used to differentiate the values of the multiplication factor and detection efficiency under specific source term. Specifically, subscript 1 indicates the parameter values when only the spontaneous fission neutron source is present, whereas subscript 2 corresponds to the values when only the (α, n) neutron source is present. Additionally, ε_{id} represents the detection efficiency for induced fission neutrons. To facilitate clarity in subsequent discussions, Eqs. (3) and (4) will be referred to as the improved "point model" equation system, apart from the original "point model" equation system represented by Eqs. (1) and (2).

III. SPATIAL EFFECT CORRECTION

A. Spatial distribution of multiplication factor and detection efficiency

The "point model" equation system utilizes lumped parameters, inherently neglecting the spatial variations of all parameters, particularly the spatial dependence of the multiplication factor and detection efficiency. To illustrate spatial dependence, we compared the radial variations of the multiplication factors M and M_L , as well as the detection efficiency, in spherical uranium-plutonium solution and plutonium metal systems at two different k_{eff} values respectively (where the



(a) Spatial distribution comparison of multiplication factors

(b) Spatial distribution comparison of leakage neutron detection efficiencies

Fig. 1. Spatial distribution comparisons about multiplication factor and leakage neutron detection efficiency along the radius in four sphere multiplication systems

higher k_{eff} corresponds to a larger sample radius). The results are presented in Fig. 1.

As shown in Fig. 1(a), for small-volume samples ($k_{eff} = 0.3$), the spatial variation of the multiplication factor is minimal. This is because the neutron mean free path is relatively long compared to the samples' size, resulting in little difference in the multiplication factor across different spatial positions. However, for large-volume samples ($k_{eff} = 0.9$), the spatial dependence of the multiplication factor becomes significant. Furthermore, the presence of a substantial amount of neutron scattering in the solution increases the probability of neutron scattering, thereby reducing the neutron mean free path and thus amplifying the spatial dependence of the multiplication factor in solution.

Fig. 1(b) demonstrates that the spatial dependence of the leakage neutron detection efficiency in the plutonium metal is negligible, showing minimal radial variation and little sensitivity to the sample volume. This behavior stems from plutonium metal's weak neutron moderating capability, which maintains a nearly uniform neutron energy spectrum throughout the sample. In contrast, solution systems display significant spatial dependence of detection efficiency, with its distribution strongly affected by sample volume. In small-volume solutions, detection efficiency increases progressively from

the center to the periphery. For large-volume solutions, neutron moderation during outward transport creates a relatively uniform detection efficiency in the central region. However, near the boundary, the energy spectra of leakage neutrons diverge, resulting in detection efficiency variations.

In conclusion, for small-volume solid samples (e.g., plutonium metal or plutonium oxides), the spatial dependences of parameters are minimal, and the "point model" can generally be applied without significant deviation. For large-volume solid samples, corrections for the spatial dependence of the multiplication factor are necessary. For solution samples, in addition to correcting for the multiplication factor, it is essential to take into account the spatial dependence of the detection efficiency.

B. Volume-weighted model

The spatial dependence of parameters compromises the accuracy of the "point model" [7]. In the "point model", the detection efficiency and multiplication factor are treated as global averages. When power operations are present in the equations, they are approximated by the "power of the mean". However, this approach does not take into account the spatial

dependence of the parameters. To address this issue, Ref. [10] introduced an improved method for large-volume plutonium metal measurements, replacing the “power of the mean” with the “mean of the power”. This refinement incorporates a correction factor g_n to acc the spatial dependence of M , defined as follows:

$$g_n = \frac{\langle M^n(\mathbf{r}) \rangle}{\langle M(\mathbf{r}) \rangle^n} = \frac{1/V \int M^n(\mathbf{r}) dV}{M^n} \quad (5)$$

Here, V denotes the total volume of the system. g_n is generally greater than 1 due to the non-uniform distribution of $M(\mathbf{r})$. For Monte Carlo simulations, the system is segmented into several subregions, allowing the integral to be approximated as the summation. Thus, the above equation can be reformulated as:

$$g_n = \frac{1}{VM^n} \sum_i v_i M_i^n \quad (6)$$

Here, the subscript i refers to subregion i , where v_i is the volume of subregion i , and M_i represents the net multiplication factor for source neutrons originating from subregion i . Since only the equation D incorporates multiple powers of the multiplication factor, modifications are exclusively applied to it.

Based on Eq. (2), the equation D of the original “point model” is refined as follows:

$$D = \frac{\varepsilon^2 g_{sf}^{240} m_{240} f_D M^2}{2} \left[g_2 \nu_{s2} + \frac{(g_3 M - g_2)}{\nu_{i1} - 1} \nu_{s1} (1 + \alpha) \nu_{i2} \right] \quad (7)$$

Analogous to this approach, the modified form of the equation D in the improved “point model” can be derived from Eq. (4):

$$D = \frac{\varepsilon_1^2 g_{sf}^{240} m_{240} f_D M_{L1}^2}{2} \left[g_{21} \nu_{s2} + \frac{(g_{31} M_1 - g_{22})}{\nu_{i1} - 1} \nu_{s1} \nu_{i2} + \alpha \frac{(g_{32} M_2 - g_{22})}{\nu_{i1} - 1} \nu_{s1} \nu_{i2} \right] \quad (8)$$

$$g_{21} = \frac{1}{V \varepsilon_1^2 M_{L1}^2} \sum_i v_i \varepsilon_{1,i}^2 M_{L1,i}^2 \quad (9)$$

$$g_{22} = \frac{1}{V \varepsilon_1^2 M_{L1}^2} \sum_i v_i \varepsilon_{id,i}^2 M_{Lid,i}^2 \quad (10)$$

$$g_{31} = \frac{1}{V \varepsilon_1^2 M_{L1}^2 M_1} \sum_i v_i \varepsilon_{id,i}^2 M_{Lid,i}^2 M_{1,i} \quad (11)$$

$$g_{32} = \frac{1}{V \varepsilon_1^2 M_{L1}^2 M_2} \sum_i v_i \varepsilon_{id,i}^2 M_{Lid,i}^2 M_{2,i} \quad (12)$$

Here, $M_{Lid,i}$ represents the leakage multiplication factor of induced fission neutron in subregion i , which replaces $M_{L1,i}$, considering the difference between the neutron energy spectra of spontaneous fission and induced fission. In Eqs. (9)-(12), we have taken into account the correction of both the multiplication factor and the detection efficiency. Eqs. (3) and (8)-(12) comprise a volume-weighted spatial-dependent model. This model is characterized by its simplicity, intuitiveness, and ease of extension. This method has demonstrably enhanced the accuracy of measurements for plutonium metal samples, as evidenced in Ref. [8–10]. Nevertheless, its applicability appears to diminish when dealing with larger-volume samples. We posit that volume weighting, while just a correction on equation form, falls short in capturing the intricacies of the physical process. Specifically, it overlooks the disparity between the induced fission source distribution and the initial source distribution. In light of these considerations, we introduce a more refined model in the subsequent section.

C. Composite-weighted model

To achieve a more rational enhancement of equation D , it is essential to delve into the physical meaning of each term in it. Neutron coincidence counting originates from two distinct sources: the multiplicity of neutrons arising from spontaneous fission events and that from induced fission events. These correspond to the first and second terms in Eq. (4), respectively (here, the second term only takes into account induced fission caused by the spontaneous fission source).

$$First\ term = \varepsilon_1^2 M_{L1}^2 \nu_{s2} \quad (13)$$

$$Second\ term = \varepsilon_{id}^2 M_{L1}^2 \frac{(M_1 - 1)}{\nu_{i1} - 1} \nu_{s1} \nu_{i2} \quad (14)$$

In the first term, $\varepsilon_1^2 M_{L1}^2$ is solely dependent on the spontaneous fission source distribution. Since this source is uniformly distributed, the correction factor g_{21} can be directly

applied, as demonstrated in Ref. [6]. In the second term, $\varepsilon_{id}^2 M_{L1}^2$ represents the coincidence count contribution from induced fission events, which depends on the induced fission source distribution. $\frac{(M_1-1)}{\nu_{i1}-1}$ denotes the number of induced fissions generated by a single initial source neutron, with M_1 related to the spontaneous fission source distribution.

Unlike the first term, correcting the second term requires more sophisticated treatment than the simple factor g_n . The

newly developed correction factor incorporates three critical aspects: (1) the induced fission reaction rate distribution, (2) the initial source distribution, and (3) the spatial variation of the detection efficiency and neutron energy spectrum differences between initial and induced fission sources, as previously discussed. The calculation equations for these two correction factors are presented below:

$$g_{L2} = \frac{1}{V \varepsilon_1^2 M_{L1}^2} \sum_i v_i \varepsilon_{1,i}^2 M_{L1,i}^2 \quad (15)$$

$$g_{M_{Ln}} = \frac{1}{V \varepsilon_1^2 M_{L1}^2} \sum_i \left(\sum_j R_{n,ij} \varepsilon_{id,j}^2 M_{Lid,j}^2 \right) v_i (M_{n,i} - 1) \quad n = 1, 2 \quad (16)$$

Here, the subscript $n = 1, 2$ denotes the initial source being spontaneous fission source or (α, n) source, respectively. The subscript id indicates induced fission neutrons, while the subscripts i, j represent the indexes of divided subregions. $R_{n,ij}$ is the proportion of induced fission reactions in subregion j to the whole system caused by initial source neutrons from subregion i ($\sum_j R_{n,ij} = 1$). $M_{Lid,j}$ is the leakage multiplication factor of induced fission neutrons in subregion j . The meanings of the other parameters are as described above.

The equation for g_{L2} aligns with Eq. (9). The physical interpretation of $g_{M_{Ln}}$ can be understood as follows: Initial source neutrons will induce fissions at different locations during transport, and the locations where induced fissions occur follow a certain probability distribution, which is described by $R_{n,ij}$. $\varepsilon_{id} M_{Lid}$ represents the expected number of detected neutrons from a single induced fission neutron. Given the spatial variations in ε_{id} and M_{Lid} across different subregions, a weighted average based on the induced fission reaction distribution is required to determine the average coincidence count per induced fission event. Furthermore, since the number of induced fissions generated by initial source neutrons varies among subregions, multiplying by $(M_{n,i} - 1)$ gives the coincidence count contribution from an initial source neutron in subregion i . The final step is a volume-weighted summation across all subregions like the volume-weighted model does.

Thus, the equation for D is obtained as follows:

$$D = \frac{\varepsilon_1^2 g_{sf}^{240} m_{240} f_D M_{L1}^2}{2} \left[g_{L2} \nu_{s2} + \frac{g_{M_{L1}} + \alpha g_{M_{L2}}}{\nu_{i1} - 1} \nu_{s1} \nu_{i2} \right] \quad (17)$$

To differentiate from the earlier volume-weighted model, Eqs. (3) and (15)-(17) are termed the composite-weighted spatial-dependent model. This model not only incorporates volume weighting but also introduces an additional weighting based on the induced fission reaction distribution. This method enhances the multiplicity model's universality and precision, however, it also increases computational costs.

IV. MONTE CARLO SIMULATION

A. Experiment methodology

To validate the correctness and accuracy of the model improvements, simulations using a three-dimensional Monte Carlo program are conducted. For ease of partitioning the sample for calculations, a spherical solution sample is utilized, which simplifies the partitioning to a single dimension. The schematic diagram of the sample and detection device is presented in Fig. 2.

The solution under investigation is a uranium-plutonium nitrate solution containing multiple isotopes of uranium and plutonium, with ^{239}Pu and ^{238}U being the predominant isotopes. The solution has a density of 1.07 g/cm^3 . The source terms consist of two types: spontaneous fission sources and (α, n) sources, with a source strength ratio of 2.15:3.04. The energy spectrum of the (α, n) source is derived from an external source term program. Given that the coincidence counting gate time is set to infinity, the gate fraction f_D is equal to 1. During the simulation experiment, the solution's radius is varied to modify its multiplication capability—a larger radius resulting in a higher multiplication factor and a larger k_{eff} . At a radius of 30 cm, the system's $k_{eff} \approx 0.9$.

A three-dimensional Monte Carlo code is employed in fixed-source mode to perform simulations, with the neutron counting rate (S) and neutron coincidence counting rate (D) calculated through the multiplicity counting function. The parameters ν_{s1} , ν_{s2} , ν_{i1} , and ν_{i2} are directly obtained from the output files (here only considering the case where the spontaneous fission source is present). The entire sample is divided radially into 1 cm-thick segments, each treated as a single subregion. For each subregion, the values of M , M_L , M_{Lid} , ε_1 , ε_2 , and ε_{id} are calculated separately. Here, M represents the net multiplication factor output directly by the Monte Carlo program, M_L is derived using Eq. (2), and ε_1 and ε_2 are computed using the following equation:

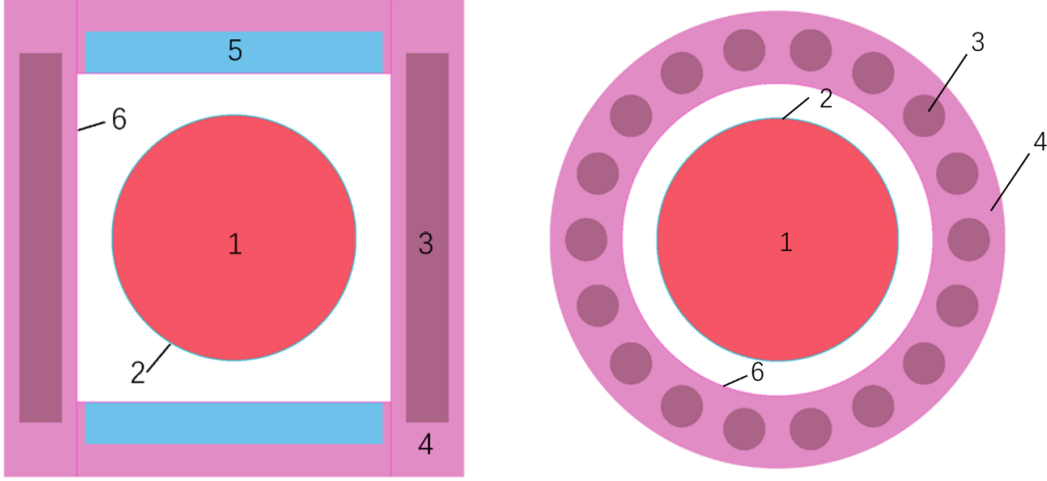


Fig. 2. Diagram of the detection system. The left figure shows the vertical cross-section, while the right figure shows the horizontal cross-section. In the diagram, 1 is the solution, 2 is the stainless-steel container, 3 is the ^3He detector (operating at 4 atmospheres), 4 is polyethylene, 5 is the aluminum (Al) layer, and 6 is the cadmium (Cd) lining.

$$\varepsilon = \frac{N_D}{M_L} \quad (18)$$

N_D denotes the number of neutrons detected from an initial source neutron, which can be obtained by tallying the capture reactions in the detector using cell tally. However, obtaining M_{Lid} and ε_{id} for induced fission neutrons is more challenging. In the “point model”, ε_{id} can be derived using the following equation:

$$\varepsilon_{id} = \frac{N_{D,on} - N_{D,off}}{M_L - (1 - p_{id,off} - p_{c,off})} \quad (19)$$

Here, the subscript “on” refers to the scenario where induced fission reactions are active, while “off” refers to the scenario where they are inactive. p_{id} is the probability of inducing fission reaction by a single neutron in the system and p_c is probability of neutron capture without fission. However, when spatial dependency is considered, this equation cannot be used to determine the spatial distribution of ε_{id} . Moreover, due to the difficulty in acquiring the induced fission

neutron spectrum and the significant computational resources required for precise calculations, a simplified approach is employed in this study: the induced fission neutron spectrum is set as a Watt spectrum, and all neutrons causing induced fission reactions are assumed as thermal neutrons, which is a reasonable approximation for solutions. By dividing the system into equidistant radial subregions and performing separate calculations, the distributions of M_{Lid} and ε_{id} can be obtained.

To validate the necessity and accuracy of the improvements, a comparative analysis is conducted for three models: the improved “point model”, the volume-weighted model, and the composite-weighted model. The accuracy of the models is evaluated by comparing the calculated effective mass of ^{240}Pu (m_{240}^{eff}) with its true value. The equations for calculating m_{240}^{eff} in the improved “point model”, volume-weighted model, and composite-weighted model are as follows:

$$m_{240}^{eff} = \frac{\frac{2D\varepsilon_2 M_{L2}(\nu_{i1}-1) - 2S\varepsilon_{id}^2 M_{L1}^2 f_D \nu_{i2}(M_2-1)}{M_{L1}^2 f_D g_{sf}^{240}}}{M_{L2}\varepsilon_2 \varepsilon_1^2 \nu_{s2}(\nu_{i1}-1) + M_{L2}\varepsilon_2 \varepsilon_{id}^2 \nu_{i2} \nu_{s1}(M_1-1) - M_{L1}\varepsilon_1 \varepsilon_{id}^2 \nu_{i2} \nu_{s1}(M_2-1)} \quad (20)$$

$$m_{240}^{eff} = \frac{\frac{2D\varepsilon_2 M_{L2}(\nu_{i1}-1) - 2S\varepsilon_1^2 M_{L1}^2 f_D \nu_{i2}(g_{32}M_2 - g_{22})}{M_{L1}^2 \varepsilon_1^2 f_D g_{sf}^{240}}}{M_{L2}\varepsilon_2 g_{21} \nu_{s2}(\nu_{i1}-1) + M_{L2}\varepsilon_2 \nu_{i2} \nu_{s1}(g_{31}M_1 - g_{22}) - M_{L1}\varepsilon_1 \nu_{i2} \nu_{s1}(g_{32}M_2 - g_{22})} \quad (21)$$

$$m_{240}^{eff} = \frac{2D\varepsilon_2 M_{L2}(\nu_{i1}-1) - S f_D \varepsilon_1^2 M_{L1}^2 \nu_{i2} g_{M_{L2}}}{M_{L1}^2 \varepsilon_1^2 f_D g_{sf}^{240} (M_{L2}\varepsilon_2 g_{L2} \nu_{s2}(\nu_{i1}-1) + M_{L2}\varepsilon_2 g_{M_{L1}} \nu_{i2} \nu_{s1} - M_{L1}\varepsilon_1 g_{M_{L2}} \nu_{i2} \nu_{s1})} \quad (22)$$

B. Results and discussion

Monte Carlo simulations are performed for five solutions of varying volumes, with the solution composition and detec-

tor device held constant. The parameters are obtained using

TABLE 1. The results of the characteristic parameters and the spatial correction factors

R/cm	10	15	20	25	30
k_{eff}	0.27586	0.51784	0.69172	0.80976	0.89095
M_1	1.2148	1.5800	2.1790	3.1988	5.1277
M_{L1}	1.0429	1.1180	1.2413	1.4507	1.8460
M_2	1.1788	1.5209	2.1045	3.0871	4.9891
M_{L2}	1.0359	1.1063	1.2264	1.4285	1.8180
ε_1	0.1652	0.1548	0.1481	0.1436	0.1388
ε_2	0.1731	0.1607	0.1526	0.1465	0.1409
g_{L2}	1.0033	1.0007	1.0043	1.0079	1.0431
$\frac{g_{M_{L1}}}{M_1-1}^*$	0.9503	0.9712	1.0307	1.1123	1.2718
$\frac{g_{M_{L2}}}{M_2-1}^*$	0.9531	0.9729	1.0287	1.1202	1.2746

* Since $g_{M_{Li}}$ is essentially the spatial correction version of the $(M_n - 1)$ term, it does not qualify as a “factor”. The strictly defined correction factor should be denoted as $\frac{g_{M_{Ln}}}{M_n-1}$.

the method outlined in Section 4.1, and m_{240}^{eff} is calculated by substituting these parameters into Eqs. (20), (21), and (22). Some characteristic parameters and the results of the spatial correction factors are presented in Table 1, where R represents the radius of the plutonium solution sphere. The five experiments cover most of the potential application scenarios, as the net multiplication factor M ranges from about 1 to approximately 5, and k_{eff} spans from deep subcritical to shallow subcritical. A comparison of parameter values across different radii reveals a general trend of sequential increase or decrease, except for g_{L2} at $R = 15$ cm. All other spatial correction factors increase with radius, reflecting the intensification of spatial dependence of parameters as the sample volume increases.

The comparison results of the three improved models are presented in Table 2. The improved “point model” demonstrates the highest accuracy for $R = 10$ cm and 15 cm. However, for larger-volume samples, its results show significant deviations, even diverging completely, highlighting the growing importance of spatial dependence with increasing volume, as expected. The volume-weighted model performs best for medium volumes, but its relative deviation trend—shifting from negative to positive and continuously increasing—suggests that its high accuracy at medium volumes may be coincidental. At $R = 30$ cm, the deviation exceeds 24%, indicating limited reliability. In contrast, the composite-weighted model exhibits relative deviations of less than 10%, all on the lower side, and outperforms the other two models for large-volume samples. This preliminary result underscores its universality and validates the improvements.

However, for small volumes, the composite-weighted model shows larger deviations than the improved “point model”. This may stem from the model's increased complexity, introducing more uncertainties during parameter ac-

quisition. Additionally, the assumption that the induced fission neutron spectrum follows a Watt spectrum for thermal neutron-induced fission may not fully align with reality, potentially introducing further deviations. Moreover, the energy spectrum's impact on multiplicity is not considered. Nevertheless, the relative deviations of all three models are minimal for small volumes, not affecting practical applications. For spherical plutonium solutions with radii less than 10 cm, spatial dependences can be neglected, and the improved “point model” can provide sufficiently excellent accuracy.

V. CONCLUSION

In order to apply to large-volume uranium-plutonium solution, we make spatial dependence corrections for “point model”. Initially, an improved “point model” suitable for solution systems is introduced. Subsequently, spatial dependence corrections are implemented based on improved “point model”: volume-weighting method is utilized by replacing the combination of powers of volume-averaged multiplication factor and detection efficiency with the volume average of their powered combinations, yielding a volume-weighted model specifically applicable for solution systems. Furthermore, by analyzing the relationship between the actual physical processes and the expression of equation D , the distribution of the induced fission source is additionally incorporated as a weighting factor, establishing the composite-weighted model. These three models are applied to calculate the effective mass of ^{240}Pu in solutions, demonstrating that the composite-weighted model outperforms the others. This confirms the composite-weighted model's robust applicability for both large and small-volume solutions. Additionally, the composite-weighted model theoretically extends the

TABLE 2. Comparison of the true value m_{240}^{eff} with m_{240}^{eff} calculated by three improved models

R/cm	$m_{240,true}/g$	$m_{240,imp}/g$	$\Delta m_{240,imp}$	$m_{240,vol}/g$	$\Delta m_{240,vol}$	$m_{240,comp}/g$	$\Delta m_{240,comp}$
10	4.34	4.36	0.46%	4.22	-2.76%	4.29	-1.15%
15	14.63	15.43	5.47%	13.54	-7.45%	13.82	-5.54%
20	34.69	46.61	34.36%	32.86	-5.28%	32.39	-6.63%
25	67.75	157.72	132.80%	68.70	1.40%	61.24	-9.61%
30	117.07	674.30	475.98%	145.57	24.34%	107.12	-8.50%

The subscript “imp” refers to the improved “point model”, “vol” signifies the volume-weighted model, and “comp” stands for the composite-weighted model.

application of “point model” and can be directly applied to plutonium-containing material systems of any volume.

The composite-weighted model proposed in this study enables the neutron coincidence counting method to determine plutonium inventory in large-volume solution systems. However, as the model becomes more refined, parameter calculations grow more complex and time-consuming, particularly

the partitioning calculations. Additionally, this model includes approximations and simplifications, such as not considering differences in ν_{i1} and ν_{i2} under different source terms and approximating the induced fission neutron spectrum as a Watt spectrum. The impact of these assumptions remains unclear. Further research on refining the model to enhance accuracy is a promising direction for future work.

-
- [1] K. Böhnel. The Effect of Multiplication on the Quantitative Determination of Spontaneously Fissioning Isotopes by Neutron Correlation Analysis. Nucl. Sci. Eng. 90(1), 75-82 (1985). doi: [10.13182/NSE85-2](https://doi.org/10.13182/NSE85-2)
- [2] D. G. Langner, J. E. Stewart, M. M. Pickrell, et al. Application Guide to Neutron Multiplicity Counting. LA-13422-M, Los Alamos National Laboratory, Los Alamos, NM (1998). doi: [10.2172/1679](https://doi.org/10.2172/1679)
- [3] I. Pázsit, A. Enqvist and L. Pál. A note on the multiplicity expressions in nuclear safeguards. Nucl. Instrum. Methods Phys. Res., Sect. A 603(3), 541-544 (2009). doi: [10.1016/j.nima.2009.03.018](https://doi.org/10.1016/j.nima.2009.03.018)
- [4] T. H. Shin, J. Hutchinson, R. Bahrn, et al. A Note on the Nomenclature in Neutron Multiplicity Mathematics. Nucl. Sci. Eng. 193(6), 663-679 (2019). doi: [10.1080/00295639.2018.1560758](https://doi.org/10.1080/00295639.2018.1560758)
- [5] Z. Shao, H. Yang, Y. Yuan, et al. Application Study on the Estimation Method of the Plutonium Solution Concentration Based on Neutron Coincidence Counting. Nucl. Sci. Eng. 41, 856-861 (2021).
- [6] M. S. Krick, W. H. Geist and D. R. Mayo. A Weighted Point Model for the Thermal Neutron Multiplicity Assay of High-Mass Plutonium Samples. LA-14157, Office of Scientific and Technical Information (OSTI), Oak Ridge, TN (United States); Los Alamos National Lab. (LANL), Los Alamos, NM (United States) (2005). doi: [10.2172/876505](https://doi.org/10.2172/876505)
- [7] S. Croft, E. Alvarez, P. M. J. Chard, et al. An Alternative Perspective on the Weighted Point Model for Passive Neutron Multiplicity Counting. (2009).
- [8] D. K. Hauck and V. Henzl. Spatial Multiplication Model as an alternative to the Point Model in Neutron Multiplicity Counting. LA-UR-14-21991, Los Alamos National Laboratory, Los Alamos, NM (2014). doi: [10.2172/1126644](https://doi.org/10.2172/1126644)
- [9] V. Henzl, K. E. Koehler and P. A. Santi. Simulation Study to Develop Spatial Multiplication Model in Neutron Multiplicity Counting. LA-UR-15-25186, Los Alamos National Laboratory, Los Alamos, NM (2015).
- [10] M. Götsche and G. Kirchner. Improving neutron multiplicity counting for the spatial dependence of multiplication: Results for spherical plutonium samples. Nucl. Instrum. Methods Phys. Res., Sect. A 798, 99-106 (2015). <https://doi.org/10.1016/j.nima.2015.07.007>
- [11] I. Pázsit and L. Pál. Multiplicity theory beyond the point model. Ann. Nucl. Energy 154, 108-119 (2021). doi: [10.1016/j.anucene.2020.108119](https://doi.org/10.1016/j.anucene.2020.108119)
- [12] I. Pázsit and V. Dykin. Transport Calculation of the Multiplicity Moments for Cylinders. Nucl. Sci. Eng. 196(3), 235-249 (2022). doi: [10.1080/00295639.2021.1973178](https://doi.org/10.1080/00295639.2021.1973178)
- [13] I. Pázsit, V. Dykin and F. Darby. Space-Dependent Calculation of the Multiplicity Moments for Shells With the Inclusion of Scattering. Nucl. Sci. Eng. 197(8), 2030-2046 (2023). doi: [10.1080/00295639.2023.2178249](https://doi.org/10.1080/00295639.2023.2178249)
- [14] S. Avdic, V. Dykin, S. Croft, et al. Item identification with a space-dependent model of neutron multiplicities and artificial neural networks. Nucl. Instrum. Methods Phys. Res., Sect. A 1057, 168800 (2023). doi: [10.1016/j.nima.2023.168800](https://doi.org/10.1016/j.nima.2023.168800)
- [15] M. S. Krick, D. G. Langner and J. E. Stewart. Energy dependent bias in plutonium verification measurements using thermal neutron multiplicity counters. International Atomic Energy Agency symposium on international safeguards. (1997). Vienna (Austria).